Magnetic-assisted Non-contact Triboelectric Nanogenerator Converting Mechanical Energy into Electricity and Light-emissions

*Long-biao Huang[a,c]f, Gongxun Bai[a,b]f, Man-Chung Wong[a,b], Zhibin Yang[a,b], Wei Xu[a], Jianhua Hao[a,b,]**

Dr. L.-B. Huang, G. X. Bai, M.-C. Wong, Z. B. Yang, W. Xu, Prof. J. H. Hao,

Department of Applied Physics, The Hong Kong Polytechnic University, Hong Kong, P. R. China

E-mail: jh.hao@polyu.edu.hk

G. X. Bai, M.-C. Wong, Z. B. Yang, Prof. J. H. Hao,

The Hong Kong Polytechnic University Shenzhen Research Institute, Shenzhen 518057, P. R. China

Dr. L.-B. Huang

Department of Applied Chemistry, Northwestern Polytechnical University, Xi'an Shaanxi 710072, P. R. China

t Dr. L.-B. Huang and G. X. Bai contributed equally to this work.

Keywords: (Triboelectric generator, light-emission, non-contact, magnetic assisted)

Due to the huge environmental issue from energy consumption of fossil fuels, harvesting green energy such as solar, wind, geothermal and ambient mechanical energy has attracted much attention not only in academic pool but also from industries.[1-5] Traditional power supply methods with wires and batteries cannot fully meet the extensive requirement of portability of microelectronics. By contrast, harvesting environment energy, such as vibration would be a potential way to address the issue.[5-9] Benefited from electromagnetic, piezoelectric, and electrostatic transduction mechanisms, a variety of generators have been fabricated, which are capable of harvesting the ambient energy into usable power such as electricity.[4, 10-14] Particularly, triboelectric nanogenerators (TENGs) as a promising approach based on the triboelectrification and electrostatic induction have attracted much attention recently.[10-14] And many applications such as portable electronics,[5, 6] photodetector,[15] electrochemical device,[16, 17] energy harvesting,[18-20] mechanical,[21] and chemical sensors,[22] have been demonstrated.

Currently, three main types of TENGs, including vertical contact-separation type,[20] in-plane sliding type,[23-25] and single-electrode type,[26] have been developed. Note that all these TENG devices have to directly contact with external mechanical motions, such as punch, harmmering, friction and so on. Unfortunately, those external mechanical motions may lead to some unavoidable and uncontrollable problems. For instance, the external mechanical motion in real world is very complex, including impact motion, rotation and so on. Under the complicated mechanical motions, the contact surface between external motion part and TENG device would be degraded by the repeated interaction under long time operation.[27] Furthermore, the electrodes served in TENG devices could be destroyed under long-time action by external mechanical stimuli. In particular, the ambient motions in applications would accompany with different mats which could directly contaminate the TENG device, especially for electrodes and surfaces with micro/nanopatterns. These problems arisen will greatly influence the performance of device, which is not favorable to practical application.[28] As far as we know, there is very limited research to overcome the obstacle[29].

Here, we propose and fabricate a novel type of magnetic-assisted non-contact TENG in which the device's contact is separated with external mechanical motion. By combining the magnetic response layer with TENG active layer, the TENG can be remotely controlled with non-contact mechanical motion via magnetic field mediation. Moreover, such a non-contact driven TENGs, has the potential to convert some complicated external mechanical motions to a simple motion of typical TENG's working mode, i.e. contact and seperation between polymer film and electrode. Furthermore, we have systematically investigated the effects of some parameters on the device's performance, including mass ratio of magnetic response layer, distance between magnetic response layer and external magnet, and the strength of magnetic field. In our previous reports,[30-32] light-emissions are observed based on piezoelectric and piezo-photonic effects. In this work, we have presented potential TENG applications in not only generation of electricity but also light-emissions. The results show a great promise in portable electronics, energy harvesting, magnetic sensor and so on.

The device structure is schematically illustrated in **Figure 1**a. The magnetic-assisted non-contact TENG consists of two parts: magnetic response layer and TENG active layer. The magnetic response layer contains PDMS/Fe-Co-Ni powder composite and ITO/PET film. The chosen Fe-Co-Ni alloys are conventional soft magnetic materials, which are widely used as industrial raw materials because of their very low coercive field and high saturation magnetization. In this structure, the PDMS/Fe-Co-Ni alloy composite functions the magnetic response of TENG when an external magnet under mechanical motion approaches towards the device. The magnetic field is absorbed by PDMS/Fe-Co-Ni layer and then the magnetic response layer is attached with the patterned PDMS film of TENG active layer. Here, the ITO/PET film is used as induced charge collector, electrode and supporting layer where the PDMS/Fe-Co-Ni composite layer is pulled away. The arced PET film acts as a separator to provide the space between PDMS layer and ITO film. Secondly, TENG active layer includes patterned PDMS film and ITO/PET film. The PDMS film with microwire pattern was duplicated and transferred from a commerical DVD disc. As shown in scanning electron microscopy (SEM) images of Figure 1b, the uniform width of PDMS microwire is around 1.5 μm which plays an important role in enhancing the output power of TENG.[14, 33-35]

The electricity generation mechanism of magnetic-assited non-contact TENG is depicted in Figure 1c-1f. Driven by magnetic force under external mechanical motion, the patterned PDMS layer will contact and separate periodically with ITO film which lead to the generation of alternating-current (AC) power. At first, without the magnetic absorption, the ITO film and patterned PDMS film separated with about 5 mm gap has no any contact with each others (Figure 1c). When the magnet drived by external mechanical motion approaches towards the device, the patterned PDMS film fully contacts the surface of ITO film (Figure 1d), due to the magnetic absorption by the PDMS/Fe-Co-Ni powder layer. When the magnet is removed, the surface of patterned PDMS film will be released with ITO film due to the arc-sharped PET film. Supposing that the PDMS and ITO layer are uncharged beforehand, the triboelectric effect will result in the negative triboelectric charges on the PDMS surface, and the corrosponding positive triboelectric charges on the ITO surface, respectively. Electrons transfer from ITO film to the patterned PDMS film due to the triboelectric series that PDMS is much more triboelectrically negative than ITO. The separation of ITO film and patterned PDMS film can generate the electric potential difference between two ITO electrodes, where electrons flow from magnetic response layer to TENG active layer (Figure 1e) and eventally an instantaneous current is created. The negative induced charges may stay on the surface of patterned PDMS film due to the insulation property of PDMS. When the magnet approaches towards the TENG device again, the potential difference between two ITO films is created to drive an instantaneous current as shown in Figure 1f. Therefore, the whole generation process of electricity in a cycle is fulfilled until magnetic response layer and TENG active layer are completely contacted again. By repeating the above processes, the magnetic-assisted non-contact TENG can continuousely provide AC electricity for potential applications.

For the subsequent comparsion of the characteristics of magnetic-assisted non-contact TENG, a standard TENG device with basic performance was fabricated using PET/ITO film and patterned PDMS/ITO/PET film. **Figure 2**a and 2b present that the open-circuit voltage (V_{oc}) and short-circuit current (I_{sc}) from the device with the size of 4 cm × 4 cm, which can achieve about 150 V and 6 μA, respectively. The separation frequency of 7 Hz was operated in the device's measurement. Accordingly, the corresponding current density is estimated to be about 0.38 μA cm^{-2}, which accords with the earlier report.[36] The resistance dependence of output voltage and current for the device is shown in Figure 2c. The output voltage increases with an increment in loading resistance, while the output current decreases when increasing loading resistance. The maximum electrical power can reach up to 0.42 mW at a load resistance of ~ 40 MO, which is similar to the previous literature[36]. Figure 2d presents that the device can lighten 10 commercial red LEDs in series without rectifier bridge or storage units.

As aforementioned, the mechanical motion from external environment can dramatically degrade various materials of TENG device, including supporting layers, electrodes and circuit materials. Moreover, direct contact between external mechanical motion and TENG device will contaminate the electrode and polymer surface, which may greatly worsen the performance of TENG device in practical applications. Therefore, how to separate the device with external mechanical motion becomes one of important issues for the realization of real TENG applications. The TENGs based on magnetic-assisted non-contact mode schematically shown in Figure 1 may provide a solution to the problems. **Figure 3** shows V_{oc} as a function of time with different mass ratio of magnetic response layer . The longer time operation of magnetic-assisted non-contact TENG is shown in **Figure S1**. The results indicate that the mass ratio (1:2, 1:3 and 1:4) of PDMS (5 g) and magnetic Fe-Co-Ni powder has an appreciable effect on the V_{oc} of the device under the separation of 10 mm gap and operation frequency of 10 Hz. When increasing the amount of magnetic Fe-Co-Ni powder, both the mass of composite and magnetic absorption force are increased. Accordingly, V_{oc} and I_{sc} were increased from about 175 V to 325 V and 6 μA to 9.2 μA, respectively (Figure 3d). At 1:1 mass ratio, the arced ITO/PET film can resist the magnetic absorption force. Due to the increased composite mass, the arced ITO/PET film has no sufficient force to pull the magnetic response layer back, which leads to the slight increment of V_{oc} and I_{sc}.

Figure 4a-e present the V_{oc} under different distance between magnetic response layer with mass ratio of 1:3 and magnet. The longer time operation of magnetic-assisted non-contact TENG is shown in **Figure S2**. The measured results indicate that the setting longer of distance between magnetic response layer and magnet leads to a obvious decrease in V_{oc}. The I_{sc} would be decreased following the longer distance between magnetic response layer as well. The mechanism responsible for the observation could be attributed to the decay of magnetic field along with increasing distance as shown in Figure 4f. Accordingly, the magnetic absorption force is influenced by changing the distance between the magnet and magnetic response layer. As shown in Figure 4f, similar change trend of V_{oc} and magnetic field strength with the distance is evident to confirm the mechanism.

According to Figure 4, the magnetic field has significant influcence to the performance of magnetic-assisted non-contact TENG. Therefore, we further investigate the influence of magnetic field strength on the parameters of device's performance. **Figure 5** presents the V_{oc} after transfering from AC to DC by an inverter as a function of magnetic field strength. In the measurement, the distance is 10 mm and mass ratio is set as 1:3. For pratical applications, the DC electricity is widely used to provide power to portable electronics. The inset of Figure 5 presents the light emission of backlight screen with the TENG contact-separation frequency of 10 Hz. As shown in Figure 5, the frequency of contact and separation between patterned PDMS film and ITO shows a similar trend of influences on the inverted V_{oc}. It implies that the decrement of frequency leads to the reduction of V_{oc}, due to the neutralization process between patterned PDMS film and ITO electrode.[37] The results show that the backlight screen can be lightened driven by the magnetic-assisted non-contact TENG. Enhancement of magnetic field strength increases the magnetic absorption force between magnetic response and non-magnetic response layers. Therefore, it is understandable that the maximum luminescence intensity of backlight screen can be observed when the device is operated under 5 kOe of magnet as shown in Figure 5d, indicating that the luminescence intensity increases when enhancing the magnetic field. The lighten backlight screen shows the potential applications of magnetic-assisted non-contact TENG in magneto-optics sensor and display.[38]

Based on the above results, the performance of magnetic-assisted non-contact TENG is influenced by contact force, orginal from magnetic absorption force, and contact area between patterned PDMS film and electrods. The magnetic absorption force between magnet and magnetic response layer is affected by the mass ratio, distance between magnetic response layer and magnet, and magnetic field strength. According to earlier reports, magnetic force between the PDMS/Fe-Co-Ni powder composite and permanent magnet can be approximately calculated as[21]

$$F_{mag} = kB\frac{dB}{dz} \tag{1}$$

where F is magnetic force, k is magnetic coefficient, z is the distance between magnet and magnetic response layer, and B is magnetic field strength. As shown in Figure 4, the magnitude of V_{oc} is significantly decreased with the increase in the distance (z) between permanent magnet and magnetic response layer due to the descrese in magnetic force (F). And the V_{oc} increases with an increment of B as show in Figure 5. On the other hand, it is well known that surface morphology of polymer in TENG may play an important role in determining the performance of device, mainly attributed to the change in contact area.[35] The triboelectric potential of TENG increases as incresing the contact area, which leads to a larger contact charging area and higher charge density (J) on the patterned polymer surface. The increment of triboelectric charge density between patterned polymer surface and electrodes leads to higher induced transferred charges of TENG, which can be expressed as

$$\delta' = \frac{\delta d \varepsilon_{rp}}{t + d\varepsilon_{rp}} \quad (2)$$

where t and d are thickness of PDMS film and gap separation between PDMS and ITO film, respectively. c_{rp} is relative permittivity of PDMS, respectively.[39] Because of the increase in the charge density (cr) and transferred charges (Q), the triboelectric potential (V) can also enhanced as

$$V = -\frac{Q}{S\varepsilon_0}\left(\frac{t}{\varepsilon_{rp}} + d\right) + \frac{\sigma d}{\varepsilon_0} \quad (3)$$

where c_0 is vacuum permittivity. Therefore, the increase of magnetic field can enhance the contact force and contact area between patterned PDMS and ITO film. As a result, higher transferred charges and triboelectric potentials are increased by reducing the distance and increasing magnetic field strength according to Equations (1)-(3), which is consistent with the measured results as shown in Figure 4 and 5. Previous reports also mentioned similar results related to the magnetic force. The magnetic-assisted TENG could be used as self-powered visualized omnidirectional tilt sensor due to the change of magnetic field.[40] By controlling magnetic field of solenoid, magnetic force between the magnetic-assisted TENG and solenoid is tunable, affecting the electrical output voltage of TENG which could reflect the change of magnetic field.[38] The results revealed that the output voltage of magnetic-assisted TENG increased with increasing of magnetic field, which is similar with our results in Figure 4 and 5. Then triboelectric charge density between patterned polymer surface and electrodes leads to higher induced transferred charges of TENG, which can be expressed as the magnetic-assisted non-contact TENG was fabricated in 1:3 mass ratio, and operated at 10 Hz with 5 kOe magnet. As shown in **Figure S3**, V_{oc} and I_{sc} can achieve up to around 275 V and 9 μA, respectively. Compared to those conventional types of TENG devices, the efficiency of our magnetic TENG devices is expected to be additionally related to the magnetic absorption of magnetic response layer..

Followed by the generation of electricity, we demonstrate the potential optical applications with the novel TENG. It is known that solid state white-light sources have been increasingly used in our daily life, including general lighting and backlight for liquid-crystal display (LCD). Up to now, solid state white-light sources are based on the light-emitting diode (LED) typically consisted of semiconductor InGaN die and yellow phosphor. All of these devices are electrically driven. In our results, the output electric power produced by the magnetic-assisted non-contact TENG is sufficient to drive some commercial electronic and optical apparatus, such as display screen and white LED lighting board. As shown in **Figure 6**a, V_{oc} can achieve up to about 150 V, further transfered from AC into DC power by using an inverter. A 5 μF capacitor was used to store the generated electrical potential from the magnetic-assisted non-contact TENG. The charged voltage can reach up to 10 V after inverted, when TENG worked at 10 Hz in 2 seconds, with 10 mm gap and 5 kOe magnet. Consequently, a commercial backlight screen with PolyU logo was immediately lighten by the stored electrical energy as displayed in Figure 6b. By integrating the magnetic-assisted non-contact TENG with white LED lighting board in Figure 6c, the whole system can be directly used for general illumination. Figure 6d illustrates that 20 white LEDs can be lighten without contact with external mechanical motion. Because of its non-contact advantage, the device provides a new possibility to develop self-powered, non-destructive, noninvasive and visualized magnetic sensor which would be more attractive than traditional one, normally restricted to the conversion from magnetic field into electric signal.[41, 42] Furthermore, it suggests that self-powered display and solid state lighting could be driven by mechanical motion or magnetic field in some situation where mechanical and/or magnetic stimuli are applicable. Visualized sensor or electronics can be developed using magnetic-assisted non-contact TENG.

In conclusion, we have demonstrated a novel type of magnet-assisted non-contact TENG. By utilization of magnetic force, the novel TENG can be separated with external mechanical motion, which may shorten the lifetime of device and degrade the device materials. We investigate the influence of mass ratio, distance between magnetic response layer and magnet, strength of magnet on the output performance. It is found that the contact force can be manipulated by controlling these parameters. And the results indicate that increasing of magnetic force will enhance the output performance of TENG. Through this work, we show the great potential application of the device for future energy harvesting, magnetic sensor as well as self-powered electronics and optoelectronics.

Experimental Section

Fabrication of triboelectric generator: The microstructure on the surface of PDMS film was transferred from the DVD disc (*i*-Pro). Firstly, the DVD cover was removed by adhesive tape and cleaned with DI water and absolute ethanol to remove residuals and dust. PDMS elastomer and cross-linker (Sylgard 184, Dow corning) in 10:1 mass ratio were mixed homogeneously and degassed about half an hour in vacuum oven at ambient temperature. After that, 5 g mixed PDMS solution was poured on the surface of DVD disc and cured at 80 ^{o}C for 60 min. After peeling off from DVD disc, the PDMS film was cut into suitable dimension and attached on the surface of ITO/PET film. The surface morphology of PDMS film was investigated by SEM (JEOL, JSM-6490).

The magnetic layer was consist of magnetic Fe-Co-Ni powder (~100 μm, ciny electric instrument, Ltd) and PDMS. The paramagnetic Fe-Co-Ni powder was homogeneously mixed with PDMS (5 g). After degassing and curing at 80 ^{o}C for 60 min, the magnetic layer was peeled off from petri dish and cut into suitable dimension. By controlling the powder weight, PDMS/ Fe-Co-Ni powder composites with different mass ratio (1:1, 1:2, 1:3, 1:4) were achieved.

Measurement of electrical performance, magnetic field and luminescence: LeCroy WaveRunner Oscilloscope (44MXI) and SR570 low noise current amplifier (Stanford Research Systems) were used to measure V_{oc} and I_{sc}, respectively. Periodical contact and separation between ITO surface and PDMS film were fulfilled by a commercial linear motor. Gaussmeter (GM05 Hirst magnetic instruments Ltd.) was used to measure the magnetic field strength. Luminescence properties were measured by Ocean Optics USB4000 CCD spectrometer with sampling time of 700 ms.

Acknowledgements

The research was financially supported by the grants from Research Grants Council of Hong Kong (GRF No. PolyU 5005/13P) and National Natural Science Foundation of China (Grant No. 11474241) and the Fundamental Research Funds for the Central Universities (G2015KY0112).

Received: ((will be filled in by the editorial staff))
Revised: ((will be filled in by the editorial staff))
Published online: ((will be filled in by the editorial staff))

[1]. Searchinger, T.; Heimlich, R.; Houghton, R. A.; Dong, F. X.; Elobeid, A.; Fabiosa, J.; Tokgoz, S.; Hayes, D.; Yu, T. H., *Science* **2008,** 319, 1238.

[2]. Hoffert, M. I.; Caldeira, K.; Benford, G.; Criswell, D. R.; Green, C.; Herzog, H.; Jain, A. K.; Kheshgi, H. S.; Lackner, K. S.; Lewis, J. S.; Lightfoot, H. D.; Manheimer, W.; Mankins, J. C.; Mauel, M. E.; Perkins, L. J.; Schlesinger, M. E.; Volk, T.; Wigley, T. M. L., *Science* **2002,** 298, 981.

[3]. Dresselhaus, M.; Thomas, I., *Nature* **2001,** 414, 332.

[4]. Wang, Z. L.; Song, J. H., *Science* **2006,** 312, 242.

[5]. Wang, S. H.; Lin, L.; Wang, Z. L., *Nano Lett* **2012,** 12, 6339.

[6]. Wang, S. H.; Niu, S. M.; Yang, J.; Lin, L.; Wang, Z. L., *Acs Nano* **2014,** *8*, 12004.

[7]. Chen, J.; Yang, J.; Li, Z. L.; Fan, X.; Zi, Y. L.; Jing, Q. S.; Guo, H. Y.; Wen, Z.; Pradel, K. C.; Niu, S. M.; Wang, Z. L., *Acs Nano* **2015,** 9, 3324.

[8]. Yang, W. Q.; Chen, J.; Zhu, G.; Yang, J.; Bai, P.; Su, Y. J.; Jing, Q. S.; Cao, X.; Wang, Z. L., *Acs Nano* **2013,** 7, 11317.

[9]. Yang, W. Q.; Chen, J.; Jing, Q. S.; Yang, J.; Wen, X. N.; Su, Y. J.; Zhu, G.; Bai, P.; Wang, Z. L., *Adv Funct Mater* **2014,** 24, 4090.

[10]. Chen, J.; Zhu, G.; Yang, W. Q.; Jing, Q. S.; Bai, P.; Yang, Y.; Hou, T. C.; Wang, Z. L., *Adv. Mater.* **2013,** 25, 6094.

[11]. Lin, Z. H.; Cheng, G.; Lee, S.; Pradel, K. C.; Wang, Z. L., *Adv Mater* **2014,** 26, 4690.

[12]. Niu, S. M.; Liu, Y.; Wang, S. H.; Lin, L.; Zhou, Y. S.; Hu, Y. F.; Wang, Z. L., *Adv. Mater.* **2013,** 25, 6184.

[13]. Wang, S. H.; Xie, Y. N.; Niu, S. M.; Lin, L.; Wang, Z. L., *Adv. Mater.* **2014,** 26, 2818.

[14]. Zhang, C.; Tang, W.; Han, C. B.; Fan, F. R.; Wang, Z. L., *Adv. Mater.* **2014,** 26, 3580.

[15]. Lin, Z. H.; Cheng, G.; Yang, Y.; Zhou, Y. S.; Lee, S.; Wang, Z. L., *Adv. Funct. Mater.* **2014,** 24, 2810.

[16]. Li, Z. L.; Chen, J.; Yang, J.; Su, Y. J.; Fan, X.; Wu, Y.; Yu, C. W.; Wang, Z. L., *Energ Environ. Sci.* **2015,** 8, 887.

[17]. Yang, Y.; Zhang, H. L.; Lee, S.; Kim, D.; Hwang, W.; Wang, Z. L., *Nano Let.t* **2013,** 13, 803.

[18]. Yang, J.; Chen, J.; Yang, Y.; Zhang, H. L.; Yang, W. Q.; Bai, P.; Su, Y. J.; Wang, Z. L., *Adv. Energy. Mater.* **2014,** 4, 1301322.

[19]. Yang, J.; Chen, J.; Liu, Y.; Yang, W. Q.; Su, Y. J.; Wang, Z. L., *Acs Nano* **2014,** 8, 2649.

[20]. Zhu, G.; Lin, Z. H.; Jing, Q. S.; Bai, P.; Pan, C. F.; Yang, Y.; Zhou, Y. S.; Wang, Z. L., *Nano Lett.* **2013,** 13, 847.

[21]. Bai, P.; Zhu, G.; Lin, Z. H.; Jing, Q. S.; Chen, J.; Zhang, G.; Ma, J.; Wang, Z. L., *Acs Nano* **2013,** 7, 3713.

[22]. Wang, Z. L., *Acs Nano* **2013,** 7, 9533.

[23]. Wang, S. H.; Lin, L.; Xie, Y. N.; Jing, Q. S.; Niu, S. M.; Wang, Z. L., *Nano Lett.* **2013,** 13, 2226.

[24]. Lin, L.; Wang, S. H.; Xie, Y. N.; Jing, Q. S.; Niu, S. M.; Hu, Y. F.; Wang, Z. L., *Nano Lett.* **2013,** 13, 2916.

[25]. Zhu, G.; Chen, J.; Liu, Y.; Bai, P.; Zhou, Y. S.; Jing, Q. S.; Pan, C. F.; Wang, Z. L., *Nano Lett.* **2013,** 13, 2282.

[26]. Niu, S. M.; Liu, Y.; Wang, S. H.; Lin, L.; Zhou, Y. S.; Hu, Y. F.; Wang, Z. L., *Adv. Funct. Mater.* **2014,** 24, 3332.

[27]. Strum, L., *Polym. Eng. Sci.* **1977,** 17, 165.

[28]. Wang, Z. L.; Chen, J.; Lin, L., *Energ Environ. Sci.* **2015,** 8, 2250.

[29]. Chen, J.; Yang, J.; Guo, H.; Li, Z.; Zheng, L.; Su, Y.; Wen, Z.; Fan, X.; Wang, Z. L., *Acs Nano* **2015**, DOI: 10.1021/acsnano.5b05618.

[30]. Wong, M. C.; Chen, L.; Tsang, M. K.; Zhang, Y.; Hao, J., *Adv. Mater.* **2015,** *27*, 4488.

[31]. Chen, L.; Wong, M.-C.; Bai, G.; Jie, W.; Hao, J., *Nano Energy* **2014,** 14, 372.

[32]. Zhang, Y.; Gao, G.; Chan, H. L.; Dai, J.; Wang, Y.; Hao, J., *Adv. Mater.* **2012,** *24*, 1729.

[33]. Fan, F. R.; Lin, L.; Zhu, G.; Wu, W. Z.; Zhang, R.; Wang, Z. L., *Nano Lett.* **2012,** 12, 3109.

[34]. Yoo, H. G.; Byun, M.; Jeong, C. K.; Lee, K. J., *Adv. Mater.* **2015,** 27, 3982.

[35]. Jeong, C. K.; Baek, K. M.; Niu, S. M.; Nam, T. W.; Hur, Y. H.; Park, D. Y.; Hwang, G. T.; Byun, M.; Wang, Z. L.; Jung, Y. S.; Lee, K. J., *Nano Lett.* **2014,** 14, 7031.

[36]. Fan, F. R.; Luo, J. J.; Tang, W.; Li, C. Y.; Zhang, C. P.; Tian, Z. Q.; Wang, Z. L., *J. Mater. Chem. A* **2014,** 2, 13219.

[37]. Fan, F. R.; Tian, Z. Q.; Wang, Z. L., *Nano Energy* **2012,** 1, 328.

[38]. Yang, Y.; Lin, L.; Zhang, Y.; Jing, Q. S.; Hou, T. C.; Wang, Z. L., *Acs Nano* **2012,** 6, 10378.

[39]. Zhu, G.; Pan, C. F.; Guo, W. X.; Chen, C. Y.; Zhou, Y. S.; Yu, R. M.; Wang, Z. L., *Nano Lett.* **2012,** 12, 4960.

[40]. Han, M. D.; Zhang, X. S.; Sun, X. M.; Meng, B.; Liu, W.; Zhang, H. X., *Sci Rep.* **2014,** 4, 4811.

[41]. Ma, J.; Hu, J. M.; Li, Z.; Nan, C. W., *Adv. Mater.* **2011,** 23, 1062.

[42]. Johnson, M.; Bennett, B. R.; Yang, M. J.; Miller, M. M.; Shanabrook, B. V., *Appl. Phys. Lett.* **1997,** 71, 974.

Figure list

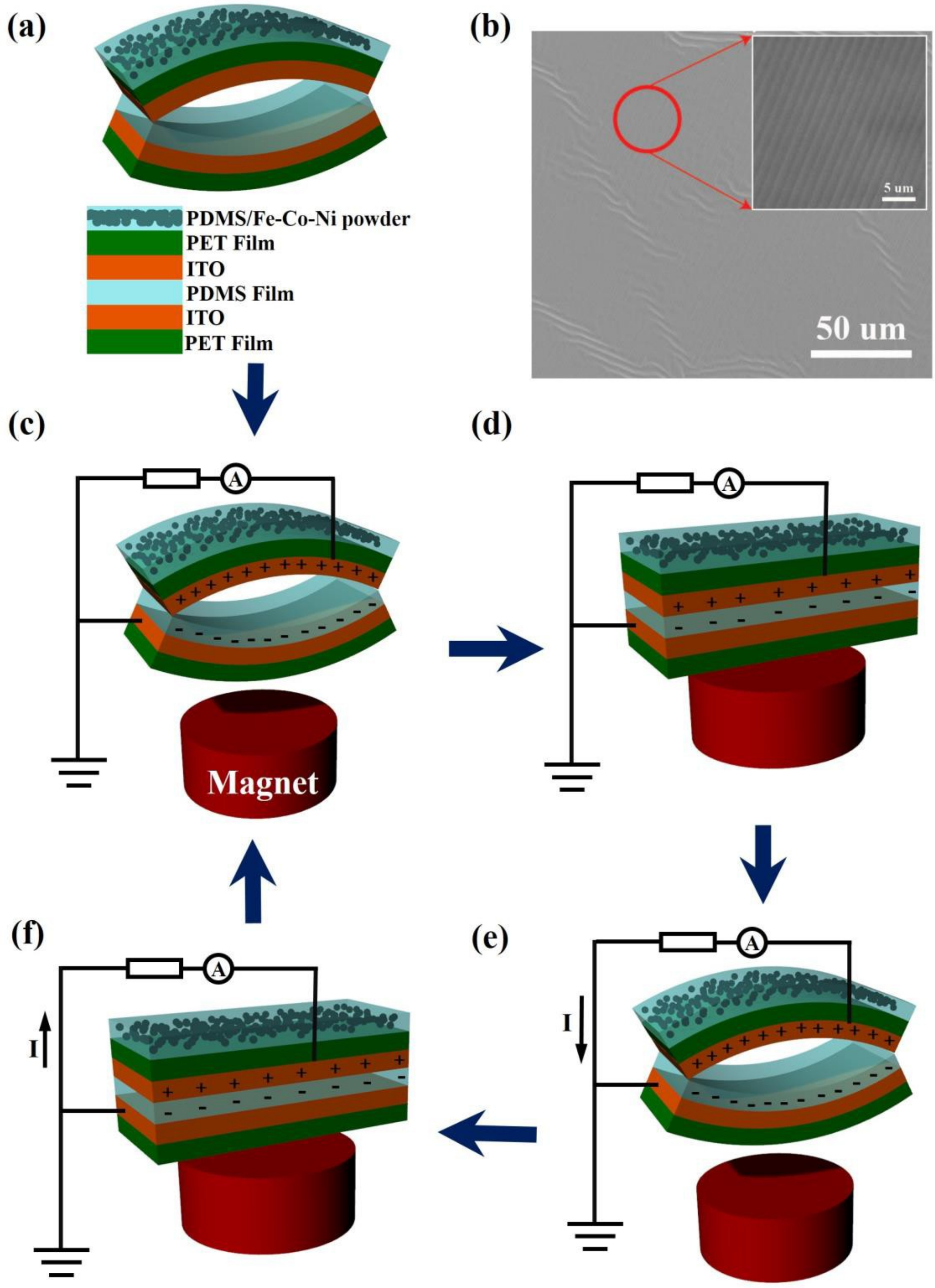

Figure 1. (a) Schematic illustration of triboelectric generator; (b) SEM image of PDMS film with microwires about 1.5 um width. Schematic illustration of working principle of TENG with photo images; (c) Original state; (d) Absorption state under the action of magnet; (e) Release state when removing magnet; (f) Absorption state under the action of magnet.

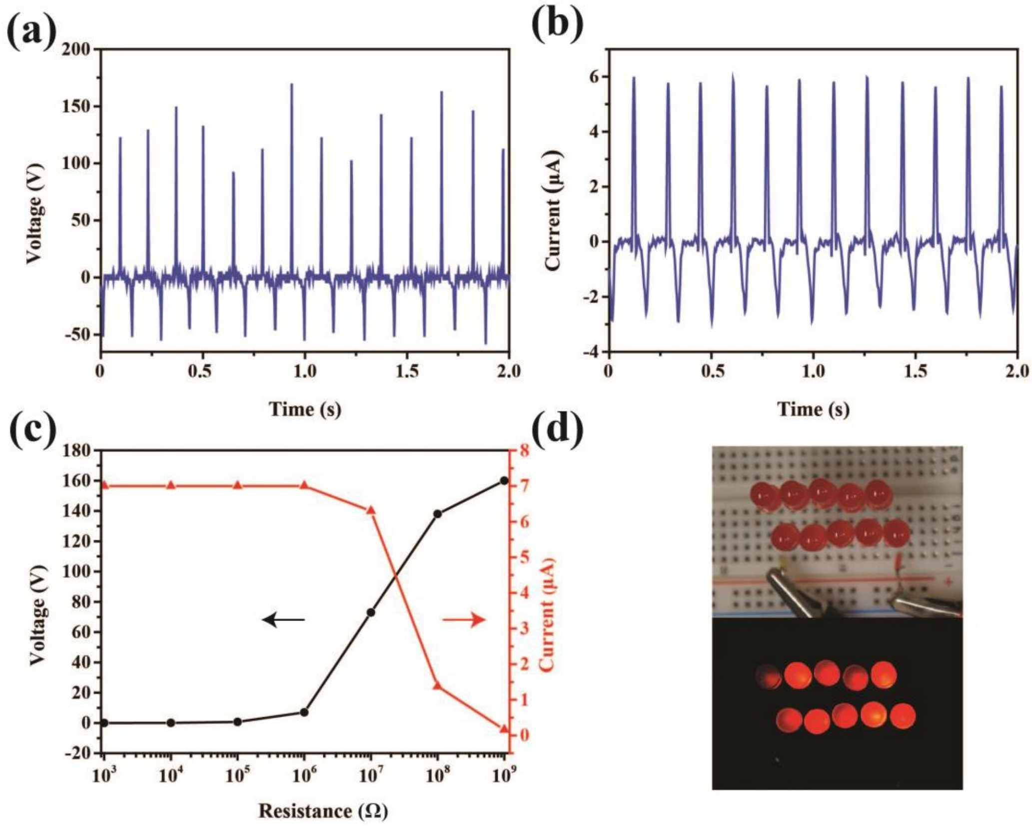

Figure 2. (a) Open-circuit voltages and (b) Short-circuit current of TENG under contact and separation with a frequency of 7 Hz; (c) Output voltage and current vs. resistance; (d) Photograph of 10 red LEDs connected in series driven by a TENG without external circuit components.

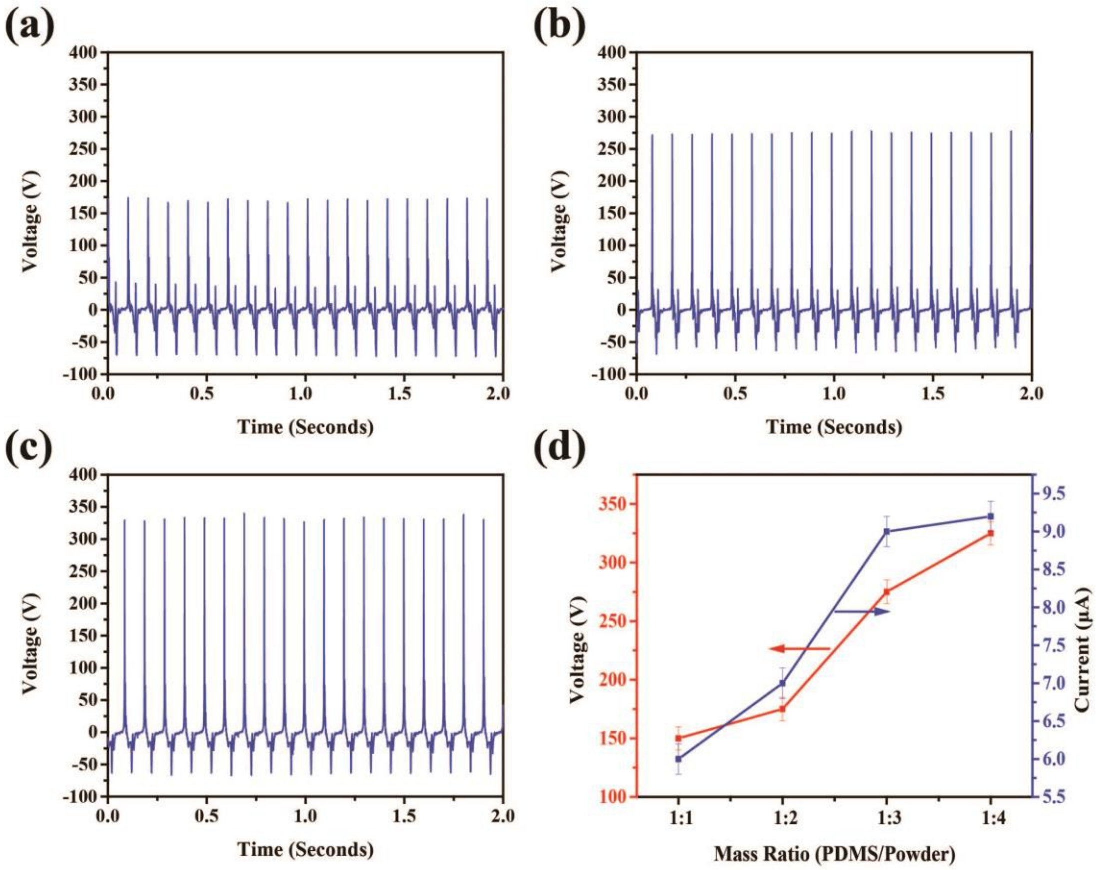

Figure 3. Open-circuit voltage as a function of time with different mass ratio of magnetic response layer in (a) 1:2, (b) 1:3 and (c) 1:4; (d) Open-circuit voltage and short-circuit current of the device versus mass ratio.

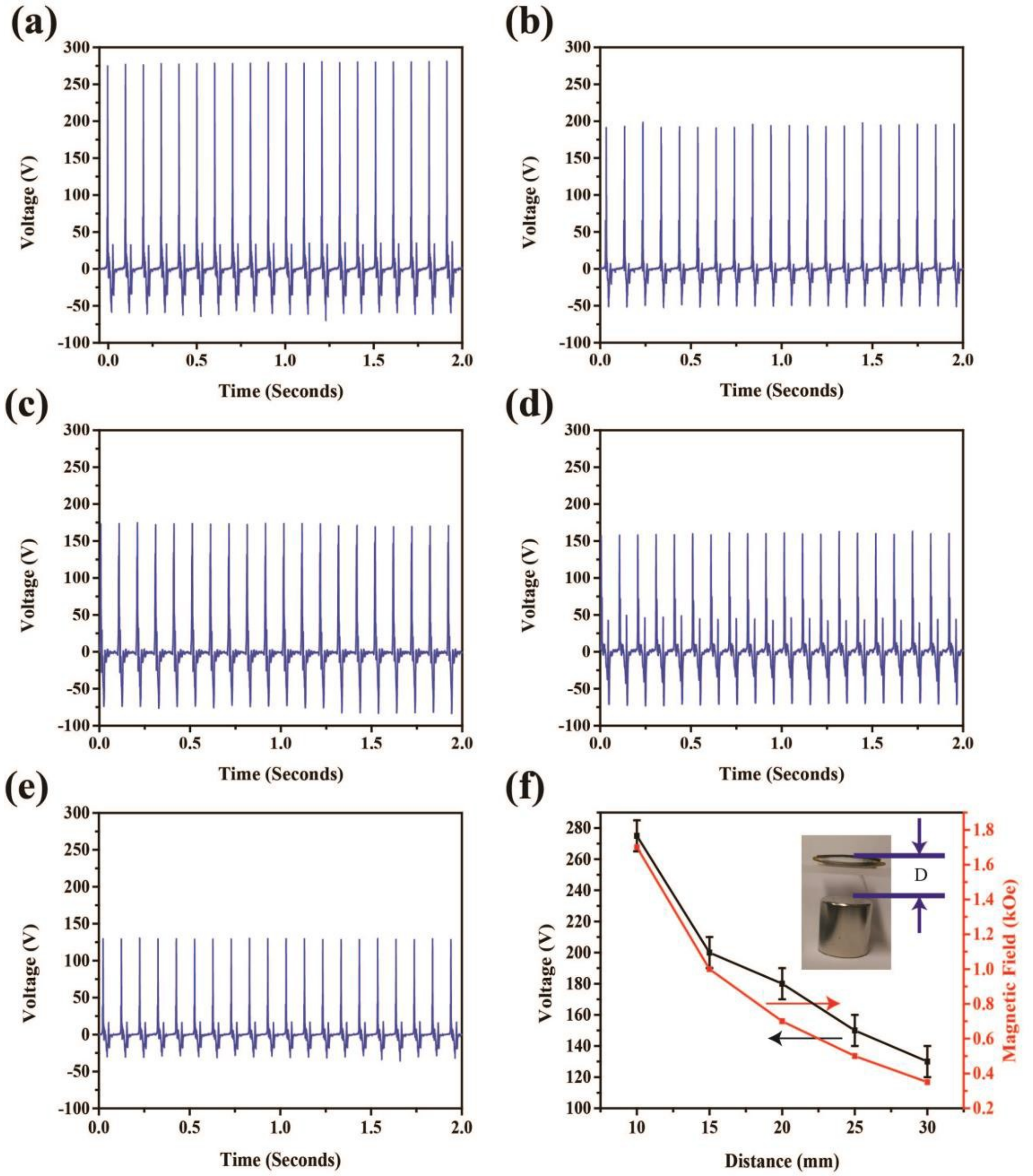

Figure 4. Open-circuit voltage versus time with different distance between magnetic response layer and magnet (a) 10 mm; (b) 15 mm; (c) 20 mm; (d) 25 mm; (e) 30 mm; (f) Open-circuit voltage and magnetic field strength versus distance between magnetic response layer and magnet illustrated in the inset.

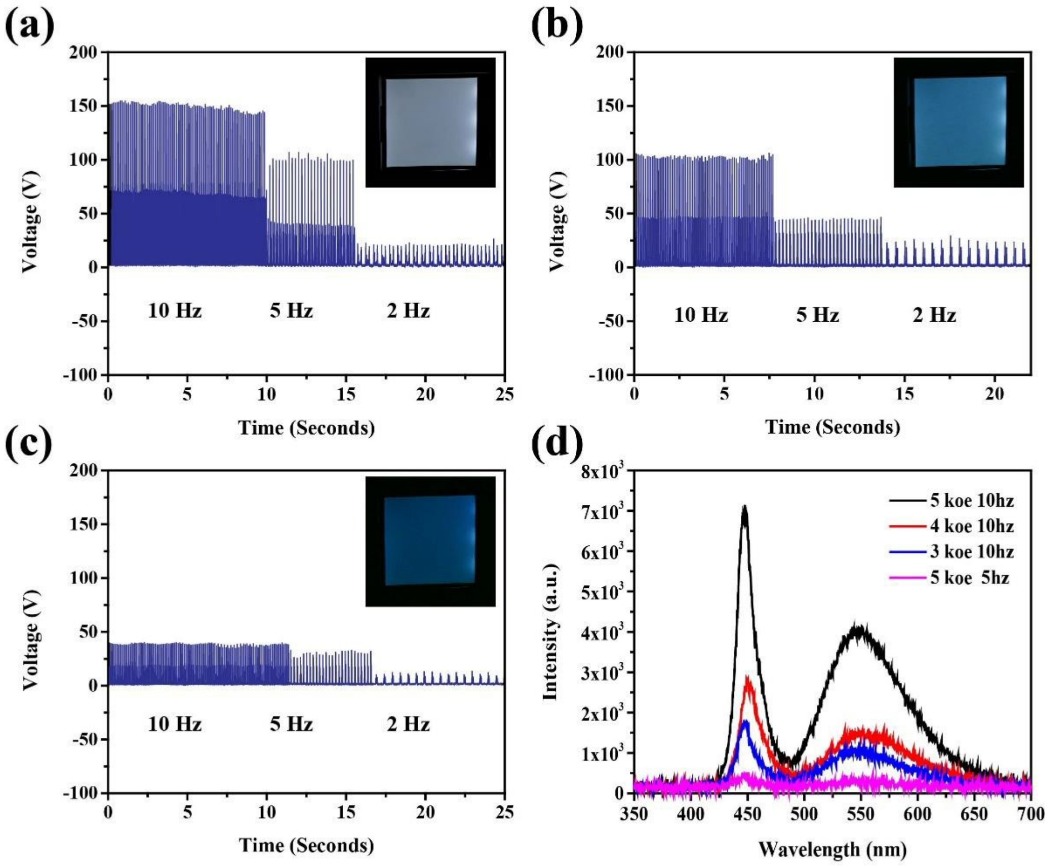

Figure 5. Open-circuit voltage versus time with different magnetic field strength of (a) 5 kOe; (b) 4 kOe and (c) 3 kOe; The inset photo shows the luminescence of lighten screen; (d) Luminescence spectrum of lighten screen under inverted DC electricity.

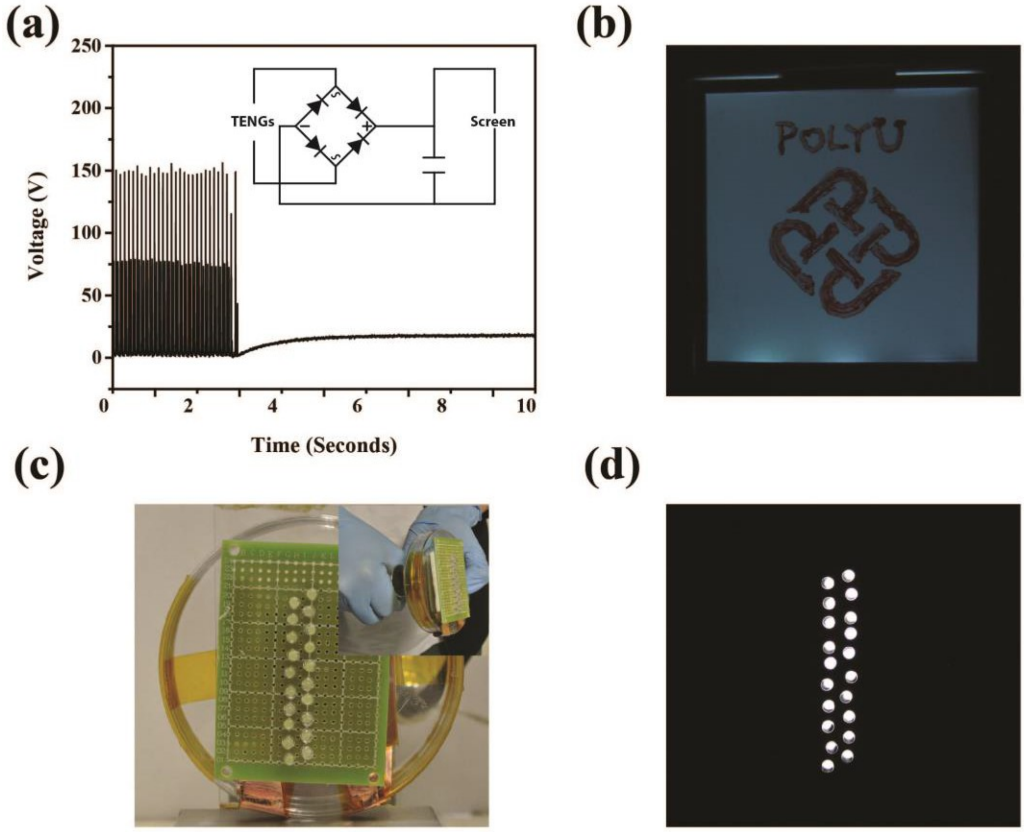

Figure 6. (a) DC voltage of TENG when inverted and connected with a capacitor at 10 Hz with 10 mm gap and 5 kOe magnet; (b) Backlight screen with PolyU logo; (c) Real sample and operation; (d) Photograph of white LED lighting panel driven by TENG.

The table of contents: Magnetic-assisted non-contact triboelectric nanogenerator (TENG) is developed by combining magnetic responsive layer with TENG device. The novel TENG is applied to harvest mechanical energy which can be converted into electricity and light-emission. The works show a promise in energy harvesting, magnetic sensor as well as self-powered electronics and optoelectronics.

Keyword

Long-Biao Huang, Gongxun Bai, Man-Chung Wong, Zhibin Yang, Wei Xu, Jianhua Hao*

Magnetic-assisted Non-contact Triboelectric Nanogenerator Converting Mechanical Energy into Electricity and Light-emissions

ToC figure